LA-UR-18-21026
Approved for public release; distribution is unlimited.

Title: Evaluation of CASL boiling model for DNB performance in full scale 5x5 fuel bundle with spacer grids

Author(s): Kim, Seung Jun

Intended for: Report

Issued: 2018-02-12

Evaluation of CASL boiling model for DNB performance in full scale 5x5 fuel bundle with spacer grids

Seung Jun Kim
Nuclear Engineering and Nonproliferation
Los Alamos National Laboratory
Los Alamos, NM 87544

Executive Summary

As one of main tasks for FY17 CASL-THM activity, Evaluation study on applicability of the CASL baseline boiling model for 5x5 DNB application is conducted and the predictive capability of the DNB analysis is reported here. While the baseline CASL-boiling model (GEN-1A) approach has been successfully implemented and validated with a single pipe application in the previous year's task, the extended DNB validation for realistic sub-channels with detailed spacer grid configurations are tasked in FY17. The focus area of the current study is to demonstrate the robustness and feasibility of the CASL baseline boiling model for DNB performance in a full 5x5 fuel bundle application. A quantitative evaluation of the DNB predictive capability is performed by comparing with corresponding experimental measurements (i.e. reference for the model validation). The reference data are provided from the Westinghouse Electricity Company (WEC). Two different grid configurations tested here include Non-Mixing Vane Grid (NMVG), and Mixing Vane Grid (MVG). Thorough validation studies with two sub-channel configurations are performed at a wide range of realistic PWR operational conditions. The test conditions for the 5x5 DNB validation are summarized as follows

- Pressure range : 160 ~ 165 bar
- Mass flux range : 1200 ~ 3600 kg/m^{2}s
- Inlet temperature: 0 ~ 50 K subcooled temperature.

To sum up, the baseline CASL boiling model (GEN-1A) demonstrates a reasonable DNB predictive capability for sub-channel applications with and without mixing vane in the spacer grid (NMVG and MVG) at maximum deviation of 16% and 26% respectively. A detailed description of the baseline CASL-boiling model (GEN-1A) is documented and preliminary results from parametric studies (mesh sensitivity, and the effect of the lift coefficient)) are also reported. While relatively poor prediction performances are presented in some ranges of operating conditions (e.g. high subcooled condition), the current DNB approach (e.g. GEN-1A) without any model calibration is believed to be a useful and reliable reference model for the 5x5 DNB analysis providing a good fundamental basis for the boiling model which helps improve next generation boiling model (GEN-1B, GEN-2).

Contents

Figures

Tables

1. Introduction

CASL THM is committed to developing and demonstrating a state of the art subcooled flow boiling DNB model with three dimensional two-fluid Eulerian based CFD approach for PWR sub-channel applications. Starccm+ version 11.04.012 is used for all DNB model validation in the present study. This milestone report includes assessment of DNB predictive capability for 5x5 fuel buddle with and without mixing vane spacer grid. Experimental DNB data is provided from the Westinghouse Electricity Company (WEC), and the reference boiling model used for the DNB validation is the CASL baseline model (GEN-1A). Over the past two years, CASL baseline boiling model has been evaluated with three different flow configurations starting from simple pipe flow to realistic 5x5 sub-channel flow configurations with and without mixing vane spacer grid. (See Figure 1). Furthermore, the current multi-step validation campaign help establish confidence in the computational DNB modeling methodology which can be used for the reactor safety application for both conventional LWR safety as well as advanced reactor design study.

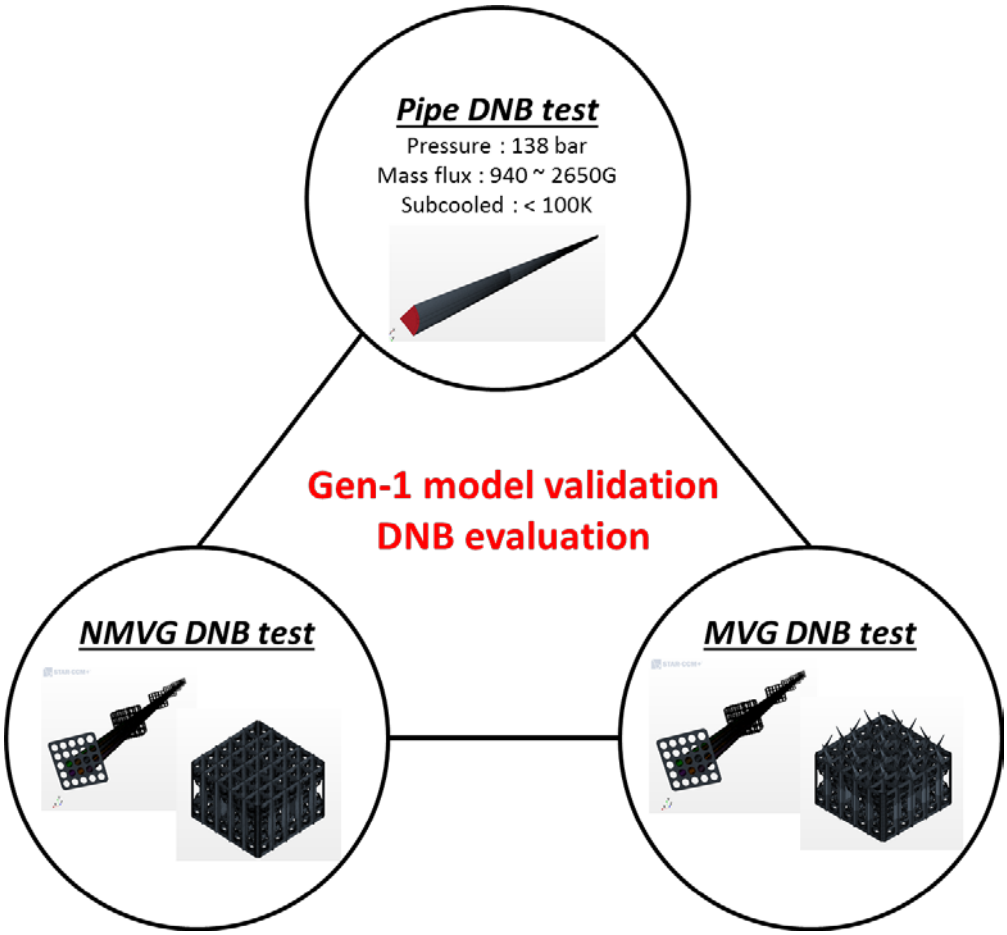

Figure 1 CASL DNB validation efforts with three flow channel configurations

The report first provides a discussion of the numeric of the GEN-1A boiling model in Chapter 2, presenting the selected boiling closure model and heat partitioning wall boiling approach. The results from two validation campaigns (e.g. Non-Mixing Vane Grid test, Mixing Vane Grid test) with the mesh sensitivity and lift coefficient effects on the DNB are briefly discussed are in Chapters 3 and 4. Finally Chapter 5 summarizes the DNB predictive capability with the baseline boiling model and discusses limitations observed from the current study and possible

directions for future development.

2. Numerical description for Gen-1A model

As documented in the previous works [1, 2], the GEN-1A model tracks the local void fraction near the heated surface to identify the inception of the DNB phenomena. In particular, the current boiling model is based on the bubbly layer theory proposed by Pei and Weisman [3]. The DNB criterion is solely based on void fraction near the wall in the computation cells. In order to accurately simulate the DNB phenomena in the CFD model, one should have a thorough understanding of closures for both multiphase interaction as well as wall boiling model for correlating the local void distribution at the wall. In fact, multiphase interaction and wall boiling models are flow regime dependent. With this in mind, the CASL baseline model (GEN-1A) has been crafted with full consideration for the subcooled boiling in high pressure applications. The detailed multiphase interaction models and boiling closure correlations selected for the DNB validation work are summarized in Table 1.

Baseline GEN-1A Boling model

- Eulerian –Eulerian based Two fluid model
- Steady RANS model for both phases with standard k-e model
- High Y+ wall treatment function applied for boundary layer
- Constant thermodynamic properties for both phase at given system pressure
- Wall heat flux partitioning approach (see detailed in Table 1)
- DNB criterion: Wall void fraction = 90% at Y+ 2000
- DNB test procedure: Incremental heat flux applied while monitoring wall temperature

Table 1. Multiphase interaction model used in the GEN-1A boiling model

Phase interaction model and Boiling closure	Selected model and correlation
Interphase momentum transfer	
➢ Lift force	No lift (C_l=0)
➢ Drag force	Tomiyama model
➢ Virtual Mass	Spherical particle model
➢ Turbulence dispersion force	Turbulent dispersion Pr=1.0
➢ Wall Lubrication force	Not Applied
Interphase mass/energy transfer	
➢ Liquid phase	Ranz-Marshall model
➢ Vapor phase	Nu=26
Interfacial Area density	Spherical particle assumption
Interaction Length Scale	Kurul-Podowski model
Wall boiling model (Heat partitioning)	
➢ Convective heat flux	Single phase turbulent convection model
➢ Evaporation heat flux	1. Bubble departure diameter model *(Tolubinski Kostanchuk correlation)* 2. Bubble departure frequency *(Cole)* 3. Nucleation site number density *(Lemmert-Chawla correlation)*
➢ Quenching heat flux	Del Valle Kenning model & Kurul-Podowski wall area fraction assumption

2.1 Two fluid based Eulerian Multi-phase CFD specification

There are three fundamental approaches to simulate two-phase flow applications in the CFD community: the volume of fluid (VOF) model, the Mixture model, and the Eulerian model. When the void fraction is high, the VOF model is recommended. However, when in the dispersed bubbly flow regime with low void fraction, the Mixture model or the Eulerian model are much more feasible to capture the two-phase phenomena with full consideration of phase change (i.e. boiling and condensation). In the Eulerian based two fluid model, there are different coupling schemes between phases for each variable. For example, the pressure is shared by all the phases, while separate continuity, momentum and energy equations are employed for each phase including liquid phase and vapor phases. The volume of each phase is calculated by integrating its volume fraction throughout the computational domain. The sum of the volume fractions is clearly equal to unity.

Mass Conservation

The conservation of mass for phase k is:

$$\frac{\partial}{\partial t}(\alpha_k \rho_k) + \nabla \cdot (\alpha_k \rho_k u_k) = \sum_{i=1}^{N} (\dot{m}_{ki} - \dot{m}_{ik}) \quad (1)$$

$$\sum_k \alpha_k = 1 \quad (2)$$

Where, α_k is volume fraction of phase k, ρ_k is phase density, u_k is phase velocity, $\dot{m}_{ki}$ and $\dot{m}_{ik}$ are mass transfer rates to and from the phase, and N is the total number of phases.

Momentum Conservation

The conservation of momentum for phase k is:

$$\frac{\partial}{\partial t}(\alpha_k \rho_k u_k) + \nabla \cdot (\alpha_k \rho_k u_k u_k) - \nabla \cdot \left(\alpha_k (\tau_k + \tau_k^t)\right) = -\alpha_k \nabla P + \alpha_k \rho_k g + M \quad (3)$$

$$M = F_D + F_{TD} + F_L + F_{VM} + F_{WL} + \sum_{i=1}^{N} (\dot{m}_{ki} u_k - \dot{m}_{ik} u_i) \quad (4)$$

Where, τ_k and τ_k^t are laminar and turbulence shear stresses, P is pressure, and M is the sum of the interfacial forces that includes drag, lift, wall lubrication, turbulence disperse force, and virtual mass force.

When it comes to the interfacial force transfer between two phases, the sum of the interfacial force (M) in Eq-(4) needs to determine the drag force (F_D), turbulence disperse force (F_{TD}), lift force (F_L), wall lubrication force (F_{WL}), and virtual mass force (F_{VM}) for the current multiphase application. As presented in the previous section, some of interfacial (interphase) momentum forces (Lift and wall lubrication) are not applied in the current DNB validation study.

Energy Conservation

The conservation of energy for phase k is:

$$\frac{\partial}{\partial t}(\alpha_k \rho_k h_k) + \nabla \cdot (\alpha_k \rho_k u_k h_k) - \nabla \cdot \left(\alpha_k \left(\lambda_k \nabla T_k + \frac{\mu_t}{\sigma_h} \nabla h_k\right)\right) = Q \quad (5)$$

$$Q = \alpha_k \frac{DP_k}{Dt} + \alpha_k (\tau_k + \tau_k^t) : \nabla u_k + \sum_{i \neq k} Q_{ki} + \sum_{(ik)} Q_k + \sum_{i \neq k} (m_{ki} h_k - m_{ik} h_k) \quad (6)$$

Where, h_k is phase enthalpy, λ_k is thermal conductivity in phase k, T is temperature, μ_t is turbulent viscosity, σ_h is turbulent Prandtl number, and Q is the interfacial heat transfer and other heat source.

Turbulence model

The realizable k-e turbulence model with high y+ wall treatment function is selected to solve flow turbulence in both phases. It is found from the previous study that the y+ value of 30~100 at the heated wall is suitable to capture the boiling heat transfer physics including interphase mass and energy transfer without any numerical instability issue. While there are still open questions on the feasibility of selected multiphase turbulence closure, the objective of the current study is only to evaluate the DNB prediction capability of the selected CASL baseline boiling model. As a separate task, one of CASL THM partner at MIT is investigating these multiphase turbulence closure model in parallel. In the present study, we follow the appropriate practice for multiphase models that is already investigated while admitting the applicability of the multiphase modeling is in active area of research in the multiphase CFD community.

Interphase interaction model

To simulate the boiling involved multiphase flows, it is necessary to establish the appropriate phase to phase interaction model due the non-trivial effects of interphase mass, momentum, and energy transfer between phases. Mass and Energy transfer in interphase interaction model are mainly modeled with Nu number correlation for each phase. Most challenging and complicated interphase interaction comes from the momentum transfer. Interphase momentum transfer can be divided into two group: drag force and non-drag force. Non-drag force models including lift and wall lubrication force are considered to be most challenging and unexplored concept in the multiphase CFD community.

Wall heat partitioning boiling model

The heat flux from the wall is divided into three parts according to a wall heat partitioning model which includes single phase convective heat, evaporative heat, and quenching heat flux. The wall dry-out factor (K_{dry}) is utilized to smoothly transition convective heat transfer mode from liquid phase to vapor phase:

$$q_w^{"} = \left(q_{Conv.liquid}^{"} + \quad q_{Evaporation}^{"} + \quad q_{Quenching}^{"}\right)\left(1 - K_{dry}\right) + q_{Conv.vapor}^{"} K_{dry} \quad (7)$$

2.2 Boundary condition specification and mesh setting

The following boundary conditions are defined to represent the corresponding DNB experimental test conditions:

- Velocity Inlet at inlet of flow channel
- Pressure outlet at outlet of flow channel
- Adiabatic wall boundary at surrounding wall (shroud)
- Uniform heat flux at 25 heat rods (6 hot rods and 19 cold rods)

Thermodynamic properties of the water and steam are determined based on the system pressure. 5x5 sub-channel model includes 5 spacer grids along with flow path in order to minimize the flow induced vibration of vertical rods. With considerations of reasonable computing model for full scale 5x5 application, we eliminated all contacts between spacer grid and rods at which a direct conjugate heat transfer between fluid and solid takes place. From sub-model tests, a conjugate modeling at contacts causes a prohibitive additional computing time.

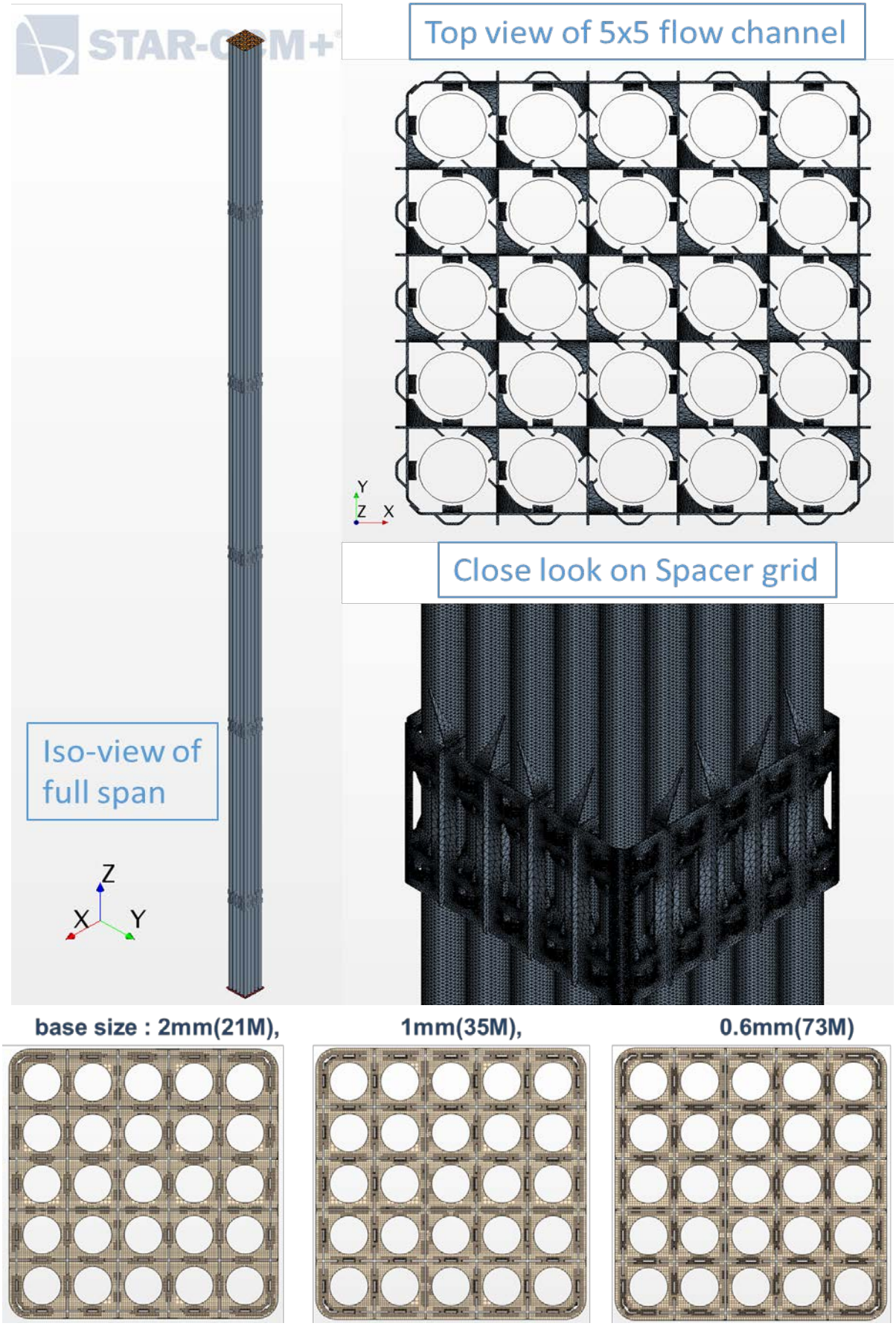

Figure 2 A visualization of 5x5 CFD domain with different views (top) and three mesh setting

A trimmer mesh scheme is applied with a layer of prism mesh at the rod surfaces. The size of trimmer mesh is controlled by the base size selection. We developed three models with different mesh controls to evaluate the grid independent study for the DNB application. (M1: 21 million cells with base size of 2mm, M2: 35 million cells with base size of 1mm, M3: 73 million cells with base size of 0.6mm). A detailed trimmer mesh setting is described below.

- Base size = 0.6mm, 1mm, 2mm (to control the bulk fluid mesh size)
- Minimum Surface size = 10% of base size
- Prism layer total thickness = 0.1 mm
- Number of Prism layer = 1
- Maximum cell size = 100% of base size

Note that the listed mesh setting is designed to produce the average Y+ value of 70 at the given inlet flow condition which should be applicable for the standard k-e turbulence model with high Y+ wall function..

3. DNB validation with 5x5 Non Mixing Vane Grid (Campaign-1)

3.1 Test matrix for the DNB validation with Non Mixing Vane Grid

Experimental DNB data at high system pressure conditions were collected from the WEC DNB report. The experimental DNB values are measured at a wide range of various system parameters such as pressure, mass flux, and sub-cooled inlet temperature. Over the various combinations of test conditions, a set of corresponding DNB measurements are used for the present validation work. While the specific experimental conditions and explicit DNB values are not presented in this report due to the Non-Disclosure Agreement, the overall range of test conditions, however, are summarized as follows

Experimental DNB with NMVG test conditions range over:

- Pressure : 70 bar ~ 165 bar
- Mass flux : 600 kg/m^{2}s ~ 3600 kg/m^{2}s
- Sub-cooled inlet temperature : ~ 150K
- Number of DNB tests : 93

The objective of the present validation is to evaluate the GEN-1A boiling model for PWR applications. Thus, a down-selected test matrix (11 selected cases) which represents typical PWR conditions is made and DNB predictions from the simulations are compared to the corresponding experimental measurements. For each of 11 cases, the DNB model with NMVG configuration are simulated to obtain an entire boiling curve history up to the inception of DNB. Qualitative and quantitative comparisons between measurement and calculation are investigated.

CFD based simulated DNB test condition includes

- Pressure range : 165 bar
- Mass flux range : 1200 kg/m^{2}s ~ 3600 kg/m^{2}s
- Sub-cooled inlet temperature : ~ 50K
- Number of DNB tests : 11

Figure 3 illustrates the maximum rod wall temperature as the heat flux is incrementally increased. The heat flux increases by 0.1 MW/m2 at every step of thermo-equilibrium condition.

Like traditional DNB experiment protocol, thermo-equilibrium is defined by monitoring outlet bulk temperature, and rod wall temperature. More precisely speaking, the rod wall temperature is a key indicator for the determination of the thermo-equilibrium condition at the given heat flux. It should be noted that the 25 rods consist of 19 cold rods and 6 hot rods with a heat flux ratio of 0.83 (heat flux at cold rods to heat flux at hot rods), and the maximum rod surface temperature is always observed one of hot rods. As shown below, the rod wall temperature tends to be fully saturated to a single value after 500 iterations in the current simulation. When the heat flux increases to 1.0 MW/m^2, the wall temperature at one of hot rods notably jumps by 40K. At this point, the DNB from the simulation is determined to be 1.0 MW/m^2, which results in 11% of deviation from the experimental DNB measurement (1.13MW/m^2).

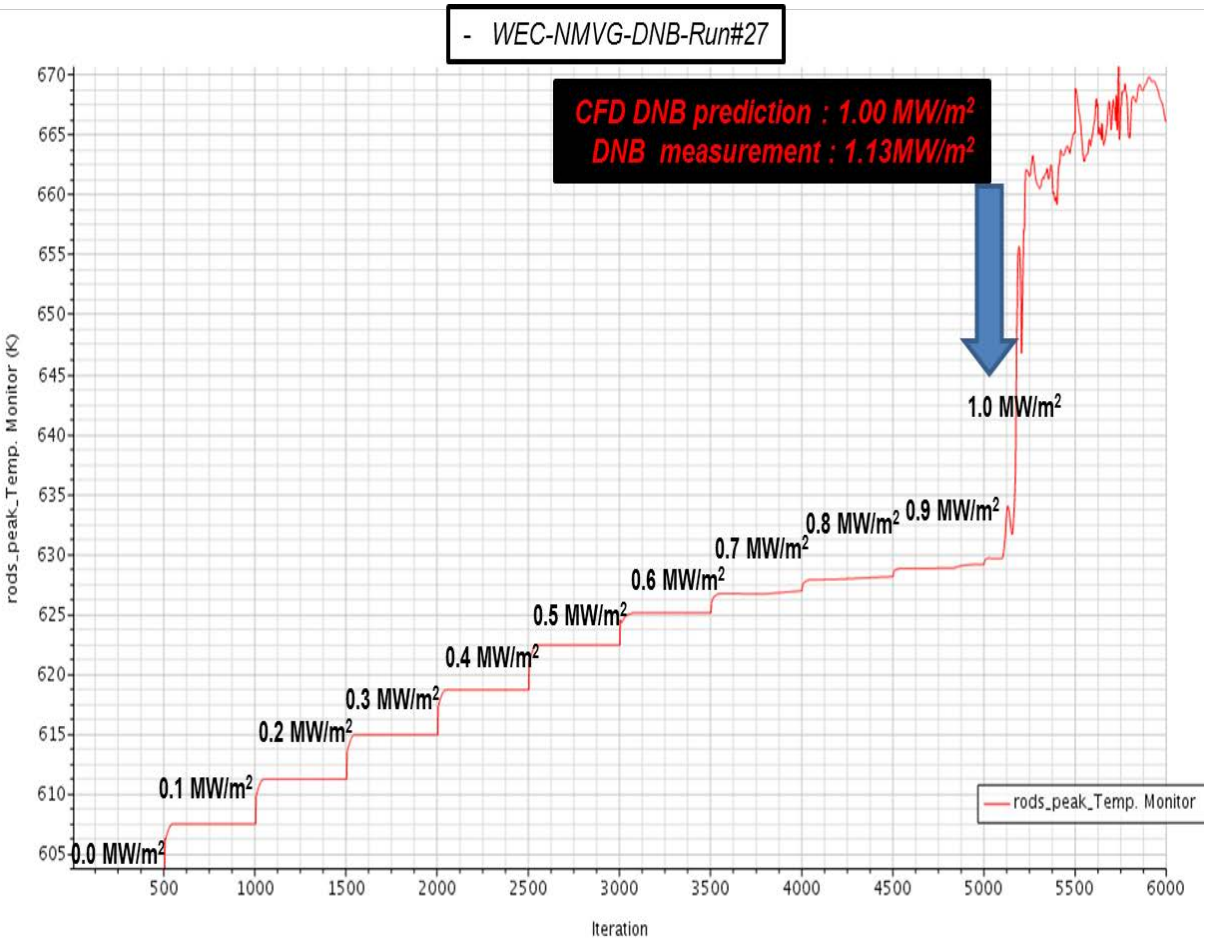

Figure 3 Wall temperature monitor with incremented heat flux up to the DNB detection.

3.2 Result of NMVG-DNB validation

To the best of the author's knowledge, the present simulation is the first full scale CFD based 5x5 subcooled flow boiling simulation up to the DNB point. The calculated DNB with only 11% of deviation from the experimental measurement appears quite promising for fuel bundle sub-channel DNB applications. More DNB tests (11 cases) are conducted with various operating condition and the qualitative DNB trend with various system conditions are illustrated in Figure 4 and Figure 5. The mass flux effect on the DNB is investigated with a range of mass flux of 1200~3600 kg/m^{2}s. Both experiments and simulations demonstrate that the DNB is delayed (or increased) as the mass flux increases. Likewise, the subcooled effect on the DNB with measured (from WEC report) and calculated (from the current test) are illustrated in the

Figure 5. It is concluded that the CFD based DNB prediction follows same trend of DNB behavior as observed in the experiments.

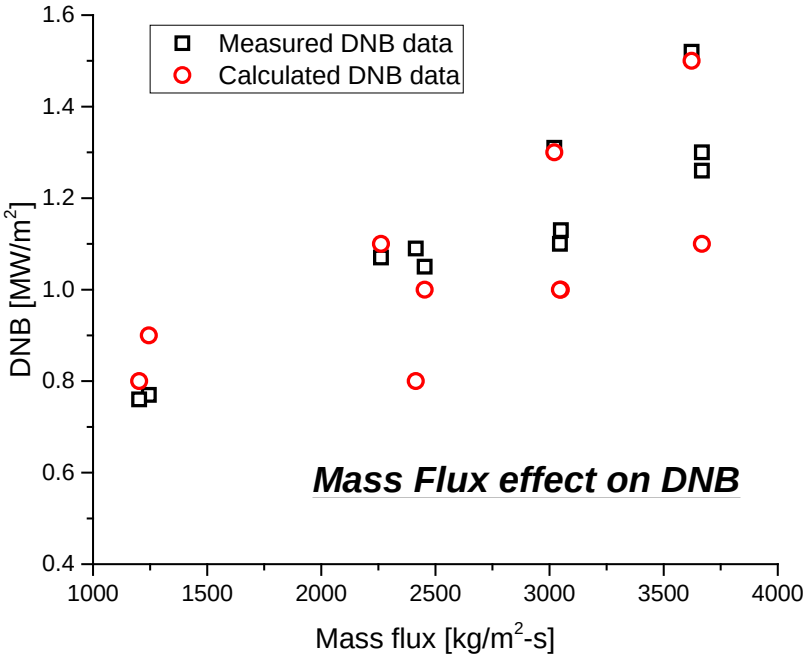

Figure 4 DNB behavior with varying mass flux (165bar, 18K < subcooled temp. < 50K)

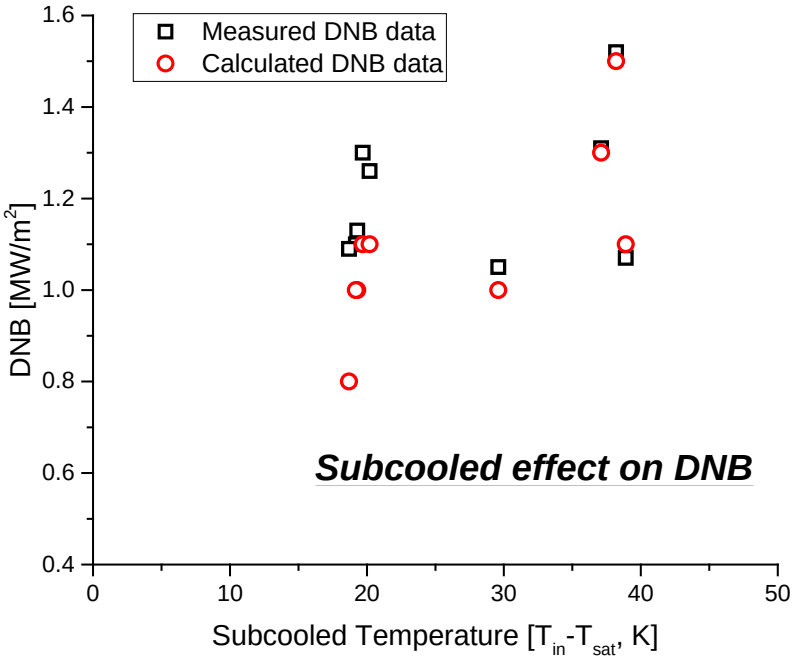

Figure 5 DNB behavior with varying subcooled temperature (165 bar, 2400 kg/m^{2}s < mass flux < 3600 kg/m^{2}s)

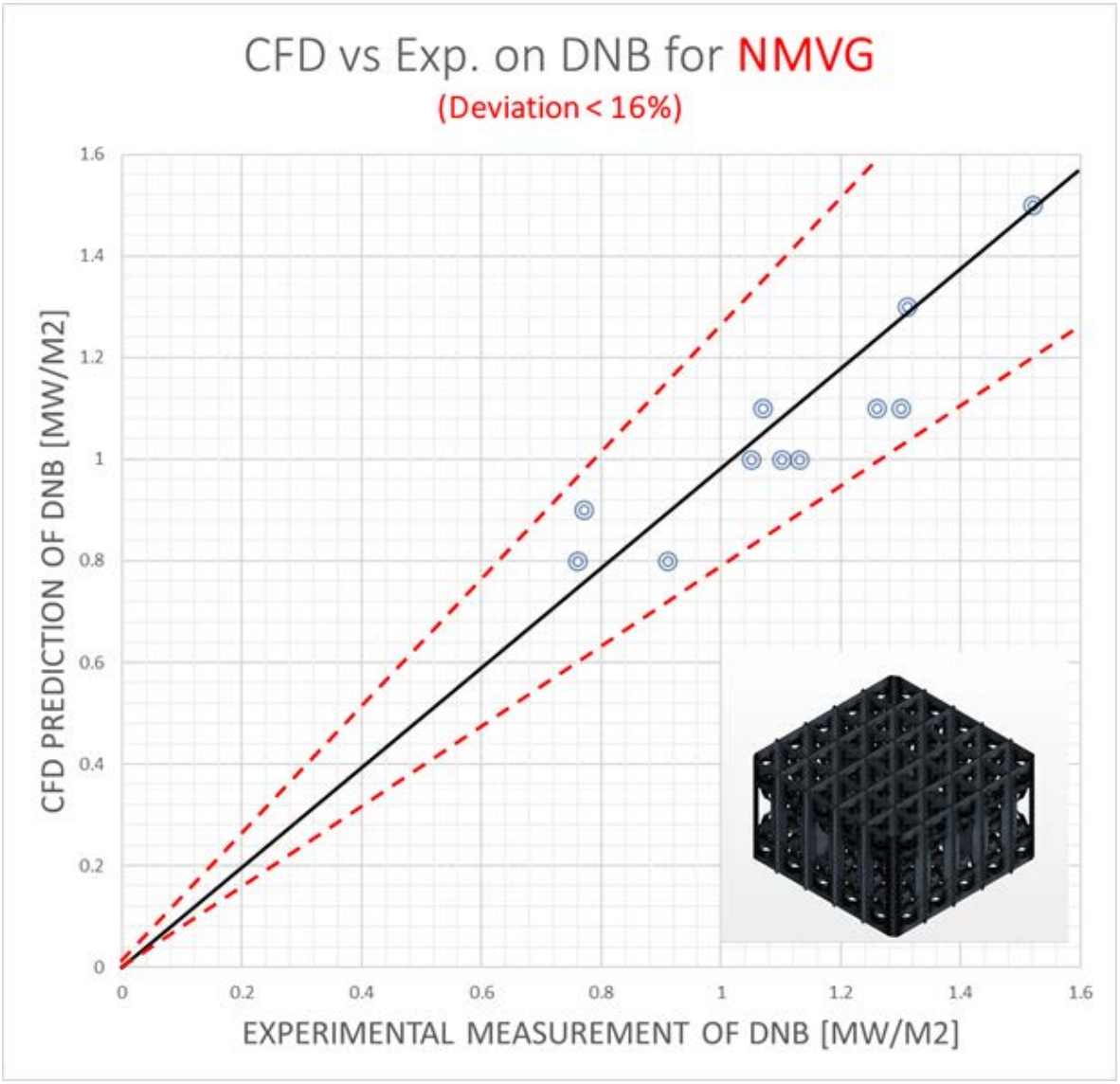

Figure 6 Predicted DNB vs measured DNB for Non Mixing Vane Grid (NMVG) configuration

With the completion of 11 DNB tests with Non-Mixing Vane Grid configuration, the calculated DNB values are directly compared to the corresponding experimental values. Red dotted line in the Figure 6 represent the deviation of 20% from the experiments. The maximum deviation among 11 test cases was 15.5%. Current level of deviation (less than 16%) for DNB application is assumed to be acceptable since the correlation based DNB prediction for sub-channel application is relatively higher. However, it should be noted that the current GEN-1A model is not universal to all operating conditions. For example, a relatively high subcooled test condition (> 50K) the deviation was increased up to 45%. It is assumed that the current boiling closure model is carefully crafted for the low subcooled boiling application at high pressure condition. Therefore, this limitation observed from the current test should be fully considered when one applies the current boiling model for different operating conditions. Nevertheless, the CASL baseline boiling model (GEN-1A) model is still feasible and highly applicable for the conventional PWR sub-channel analysis.

4. DNB validation with 5x5 Mixing Vane Grid (Campaign-2)

An identical DNB model using GEN-1A with Mixing Vane Grid geometry is constructed to evaluate its predictive capability in a more complicated (i.e. mixing vane) configuration.. With same test protocol, the DNB is detected by monitoring the maximum rod wall temperature at incrementally increasing heat flux conditions. Figure 7 demonstrates the rod surface temperature with applied heat flux condition at the baseline operating condition (e.g. MV-DNB-Run#27). As shown below, the experimental DNB value is measured at 1.22 MW/m^2 and the temperature excursion (i.e. DNB) is monitored at 0.9 MW/m^2. The deviation between measurement and calculation is approximately 26%. It is interesting to note that the predictive capability with mixing vane grid case become relatively poor compared to the non-mixing vane case (~16%). It is considered that dynamic mixing phenomena occurring downstream of the mixing vane are not captured with the current boiling closure. This discrepancy can be improved by conducting more closure parameter sensitivity studies.

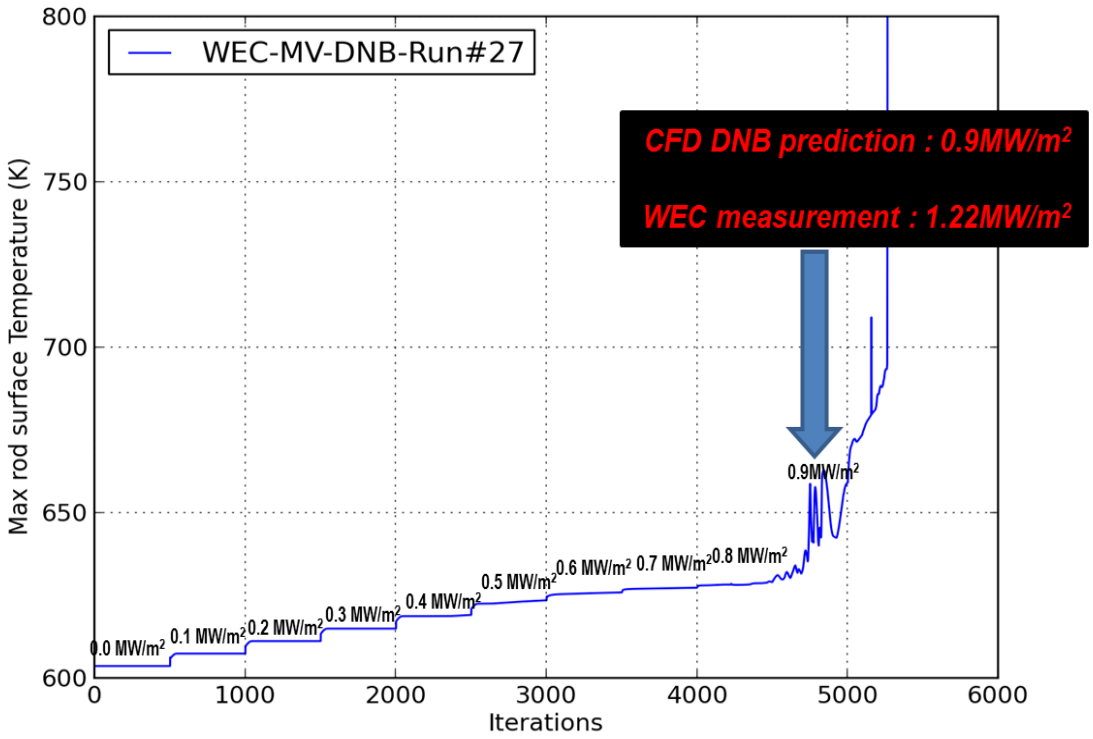

Figure 7 first Mixing Vane Grid DNB validation test result

In addition, an analysis to identify local (potential) DNB location is investigated from the post-processing the CFD simulation at the pre-DNB condition. Since the current DNB simulation accumulates the history of the boiling heat transfer scenarios encompassing single phase convective heat transfer, transition to nucleation heat transfer, and up to the DNB point (0.9MW/m^2). Pre-DNB condition case file (e.g. 0.8 MW/m^2) is further evaluated by visualizing the surface wall temperature and high void fraction distribution. As expected, the simulated DNB test can provide more comprehensive understanding on the detailed wall boiling characteristics and local information for detailed sub-channel analysis. For example, identification of the potential DNB location and mixing vane effect on the DNB are good exemplary analysis that only CFD based DNB model can provide.

As shown in Figure 8, high void area is visualized using iso-surfaces in the post-processing of CFD analysis. Most of high void is observed at the downstream of the fifth mixing vane spacer where the rods wall (6 hot rods is only illustrated in the Figure 8) already exceeds the saturation temperature. As expected, the high void is only observed near at the hot rods only. In fact, the current DNB simulation can provide not only the systematic critical safety response such as DNB value, also axial and radial local DNB related information (e.g. detailed rod wall temperature and axial location of the potential DNB spot as the heat flux is getting close to the critical value). Since the DNB is local phenomenon in two phase system, aforementioned analysis could provide considerable insight for reactor sub-channel safety study.

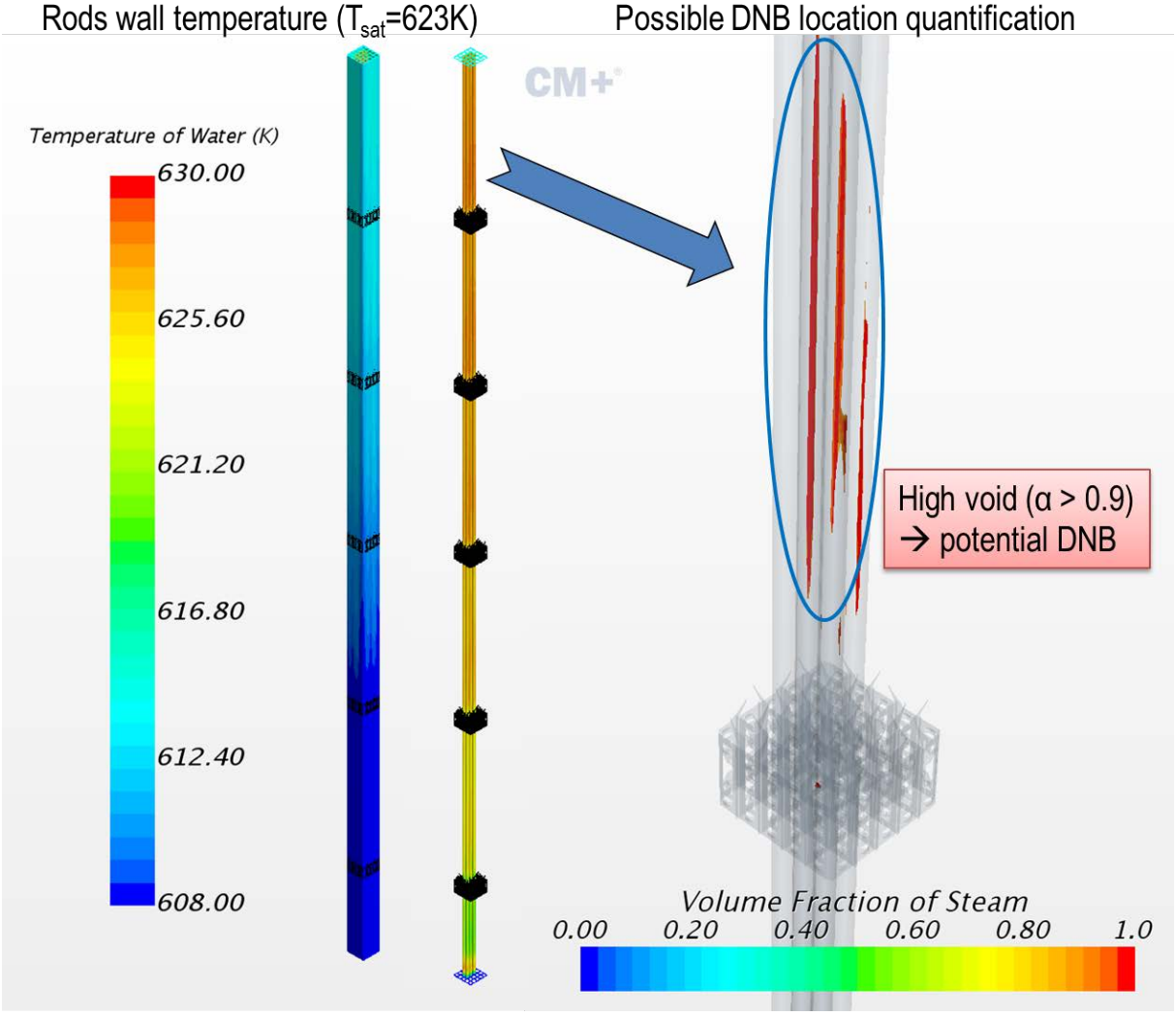

Figure 8 Rod wall temperature (left) and a potential DNB location quantification (right)

At the similar operating condition (P=165bar, 3000 Kg/m^{2}s, ~ 20K subcooled inlet), two spacer grid configurations (NMVG vs. MVG) are compared to evaluate the mixing vane effect on the potential DNB location detection. High void fraction (α>0.8) is visualized at the Pre-DNB condition. Interestingly, Figure 9 notably illustrates that the high void fraction area (i.e. potential DNB location) is further pushed upward with Mixing Vane Grid case. These comparative visualization of high void fraction indicates that the mixing vane is effectively stirring the turbulence at the downstream of the spacer grid and pushing the potential DNB location further downward in the flow direction. The mixing effect between two flow channel configurations is clearly illustrated by visualizing the stream line (See Appendix A).

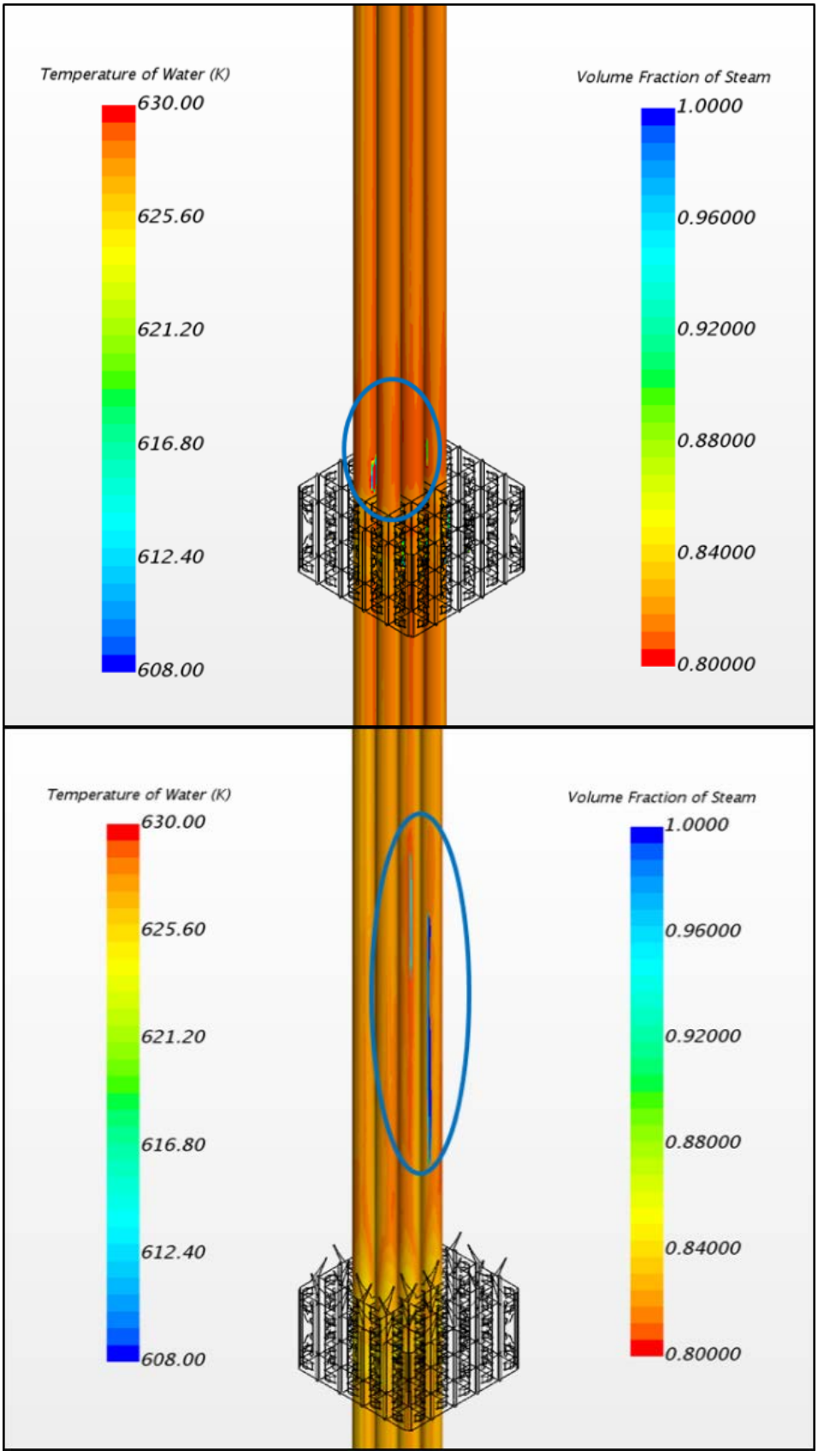

Figure 9 Potential DNB location (blue circled) with NMVG (top) and MVG (bottom).

4.1. Grid sensitivity study for DNB

In general, the grid sensitivity study is a key validation process for high fidelity CFD modeling. As discussed by many previous researcher, grid sensitivity study is usually performed by refining the mesh size and monitoring the characteristic parameter that numerical model is mainly seeking for (i.e. pressure drop, temperature, velocity profile). This type of validation process is also known as numerical uncertainty quantification (i.e. discretization error). In fact, performing a well-designed mesh sensitivity study is not an easy task because it usually requires heavy computing cost and non-trivial modeling effort. Majority of grid sensitivity study are focusing on the grid (i.e. mesh) refinement in which the core physics of interest takes place. Unlike the conventional single-phase grid sensitivity study approach, however, the present study presents the boiling heat transfer physics near at heating surface at which many empirical boiling closures are coupled with.

Some of boiling closure correlations such as bubble departure diameter and bubble departure frequency appear instability issue with fine mesh near at the wall where bubbles are generated. In addition, the multiphase turbulence model is still questionable when the fine mesh is applied at near wall. With these considerations in mind, the GEN-1A boiling model is intentionally utilizing the standard k-e model with high y+ wall treatment feature to circumvent those wall boundary mesh issue.

To evaluate the grid sensitivity, we configure three different meshes by only controlling the bulk mesh size while maintaining the boundary wall mesh specification (e.g. 30< Y+ < 100). Bulk mesh size is controlled by the base size selection in the trimmer mesh setting. Three base sizes (M1: 2mm, M2: 1mm, and M3: 0.6mm) lead to three models with the total cell count of 21M, 35M, 73M respectively. It should be noted that additional group of mesh sensitivity was conducted by control wall boundary layer specification and found stability issue as the wall boiling model started kicking in as the applied heat flux increase.

Three established models with M1, M2, and M3 are used to validate wall boiling simulation up to the DNB condition. As shown in Figure 10, a temperature excursion takes place at similar heat flux conditions. The predicted DNB value with three models are 0.9 MW/m2 (M1 and M2) and 1.0 MW/m2 (M3). The measured DNB value for the corresponding test condition is 1.22 MW/m2. For this specific case, fine mesh M3 demonstrate relatively improved DNB predictive capability compared to the coarser mesh M1 and M2. In addition, fine mesh (M3) present a distinctive temperature excursion (sudden temperature rise when the critical heat flux is applied) while less distinctive temperature jump characteristics are observed in other models (M1, and M2). However, the result from the extended grid sensitivity study with a wide range of test conditions (see Figure 11) indicates that the mesh refinement does not appreciably improve the DNB prediction performance.

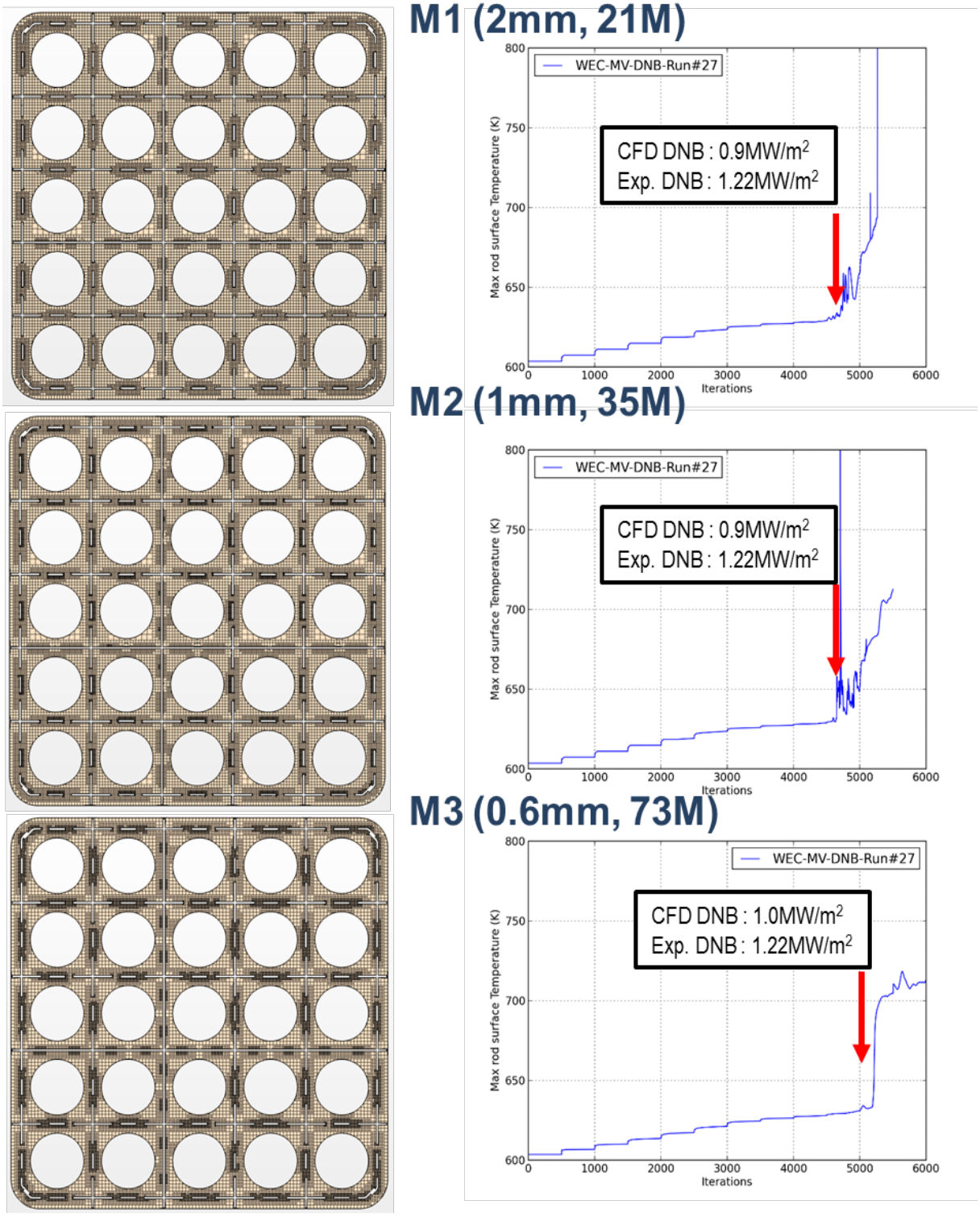

Figure 10 Mesh refinement (M1,M2, and M3) effect on DNB detection

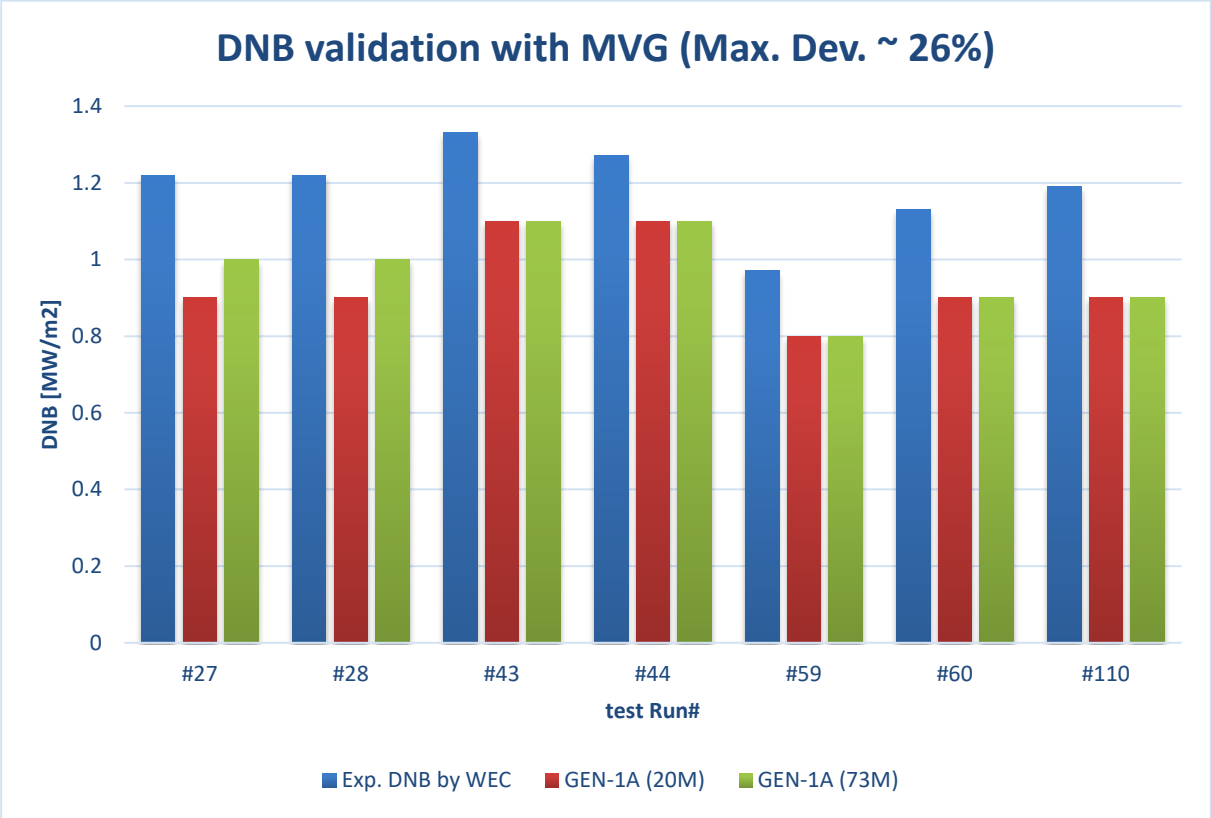

Figure 11 DNB validation results with two different mesh refined models (Blue: experiment, Red: CFD prediction with M1 mesh, Green: CFD prediction with M3 mesh).

As shown above, two DNB models with M1 (20 million cell) and M3 (73 million cell) are tested and compared to the experimental measurements. 7 different operating conditions are applied in this validation study. Interestingly, it is found that the sensitivity of the prediction performance with refining mesh size in the bulk fluid zone is not pronounced except for the highly subcooled conditions (run#27, run#28). In fact both M1 and M3 mesh demonstrate similar predictive capability for the mixing vane spacer grid configuration.

The results from the current mesh sensitivity study could provide a practical DNB modeling guideline for the fuel bundle sub-channel application. Furthermore, mesh refinement strategy for high fidelity DNB modeling is still ongoing as the best practice guideline for the GEN-1A boiling is being established and improved. However, it should be reiterated the mesh requirement for the phase change multi-phase CFD simulations is not easy to define since the boiling physics in the computation domain is interconnected to a non-trivial amount of the empirical based closure model. So here, we are not trying to conclude a definitive mesh requirement for the DNB application, but suggesting that the mesh setting used in the current study is desirable to produce good predictive capability with reasonable computing cost.

4.2. The effect of Lift coefficient on DNB calculation

As discussed in the previous section, determination of the DNB thoroughly relies on the void fraction distribution near the heated rod surface. So, the appropriate void fraction calculation is critical to improve the DNB prediction in boiling model. The void fraction distribution is determined by the interphase momentum transfer in the two-fluid Eulerian solver. As shown in

the equation 3 and 4, the momentum related force terms are evaluated by the selected interfacial momentum transfer correlation. Among 5 different force terms (i.e. drag, lift, virtual mass, turbulence dispersion, wall lubrication) lift and wall lubrication force are assumed to be the most dominant lateral forces to accurately calculate the void fraction near the heated rod surface. For the simplicity and robustness of the baseline CASL boiling model, the wall lubrication force becomes inactive and the lift force is set to a constant value (baseline reference is set to be zero) instead of applying an Eotwos number-based correlation such as the Tomiyama model.

To evaluate the lift coefficient effect on the DNB prediction, a group of DNB tests were designed and conducted. Three reference meshes are used and five different lift coefficients are defined as -0.05, -0.025, 0 (default), +0.025, and +0.05 respectively. In general, a positive lift coefficient implies the net lift force on the bubble towards the bulk fluid, in other words basically pushing the bubble away from the wall, which in turn delays the DNB since the void fraction at the wall is under-estimated. On the contrary, the reverse bubble force mechanism is applied when the negative lift coefficient is entered. So, the bubble is pushing toward to the wall which leads to high void fraction at the relatively low heat flux, which in turn triggers DNB at the lower heat flux condition.

Figure 12 illustrates the effect of the lift coefficient on the DNB prediction. At a default lift value (C_l= Zero, CASL baseline GEN-1A model described in Table1) the DNB is detected at the heat flux of 0.9MW/m^2. Delayed DNB values (i.e. temperature excursion detection at the higher heat flux, 1.0 MW/m^2) are observed at the positive lift coefficients (i.e. C_l= +0.025, +0.05), and reduced DNB values (i.e. temperature excursion DNB detection at the lower heat flux, 0.8MW/m^2) are observed. As clearly shown in Figure 12, it is believed that the current boiling model approach for the 5x5 DNB application is susceptible to the lateral void fraction distribution model such as lift force correlation. To achieve the high fidelity DNB model, it is firmly recommended that more practical and appropriate lateral interphase momentum transfer modeling (i.e. lift and lubrication force model) should be further investigated.

The effect of the lift coefficient on the DNB performance with three different meshes are further investigated and reported in the Appendix B. However, the overall lift effect on DNB is observed in a similar manner with slight deviations between the three meshes.

It should be reiterated that the CASL baseline DNB model (GEN-1A boiling) intentionally does not implement the lift and wall lubrication model, but focuses on the robustness and maturity of the DNB application. In parallel, the improved CASL baseline DNB model (GEN-1B model, or GEN-2) is being investigated by one of CASL THM partner groups at MIT. Those improved DNB model can be further investigated based on the lesson learned from the current study.

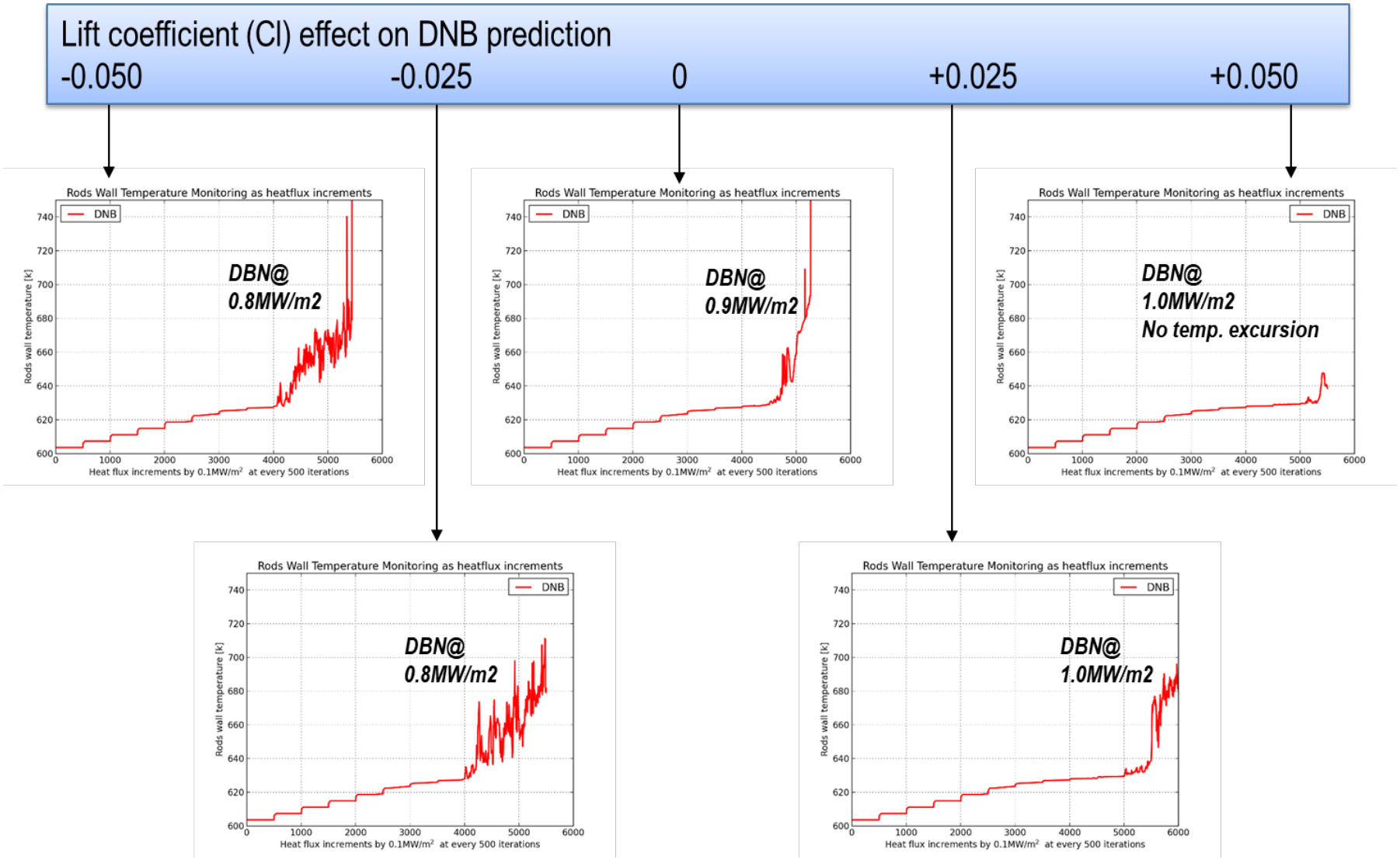

Figure 12 Lift coefficient effect on DNB with M1 mesh

4.3 Result of MVG-DNB validation

CFD based simulated MVG-DNB test conditions includes

- Pressure range : 165 bar
- Mass flux range : 1200 kg/m^2-s ~ 3600 kg/m^2-s
- Sub-cooled inlet temperature : ~ 30K
- Number of DNB tests : 7

Unlike the results from the previous validation campaign (Non-Mixing Vane Grid), the DNBs predicted from the CASL boiling model are under-predicted compared to the experimental measurements. The maximum deviation presents approximately 26%. It is believed that the under-prediction of DNB attributes to the mixing effect from the spacer grid configuration which may require further improvement of baseline CASL boiling model for the Mixing vane sub-channel application.

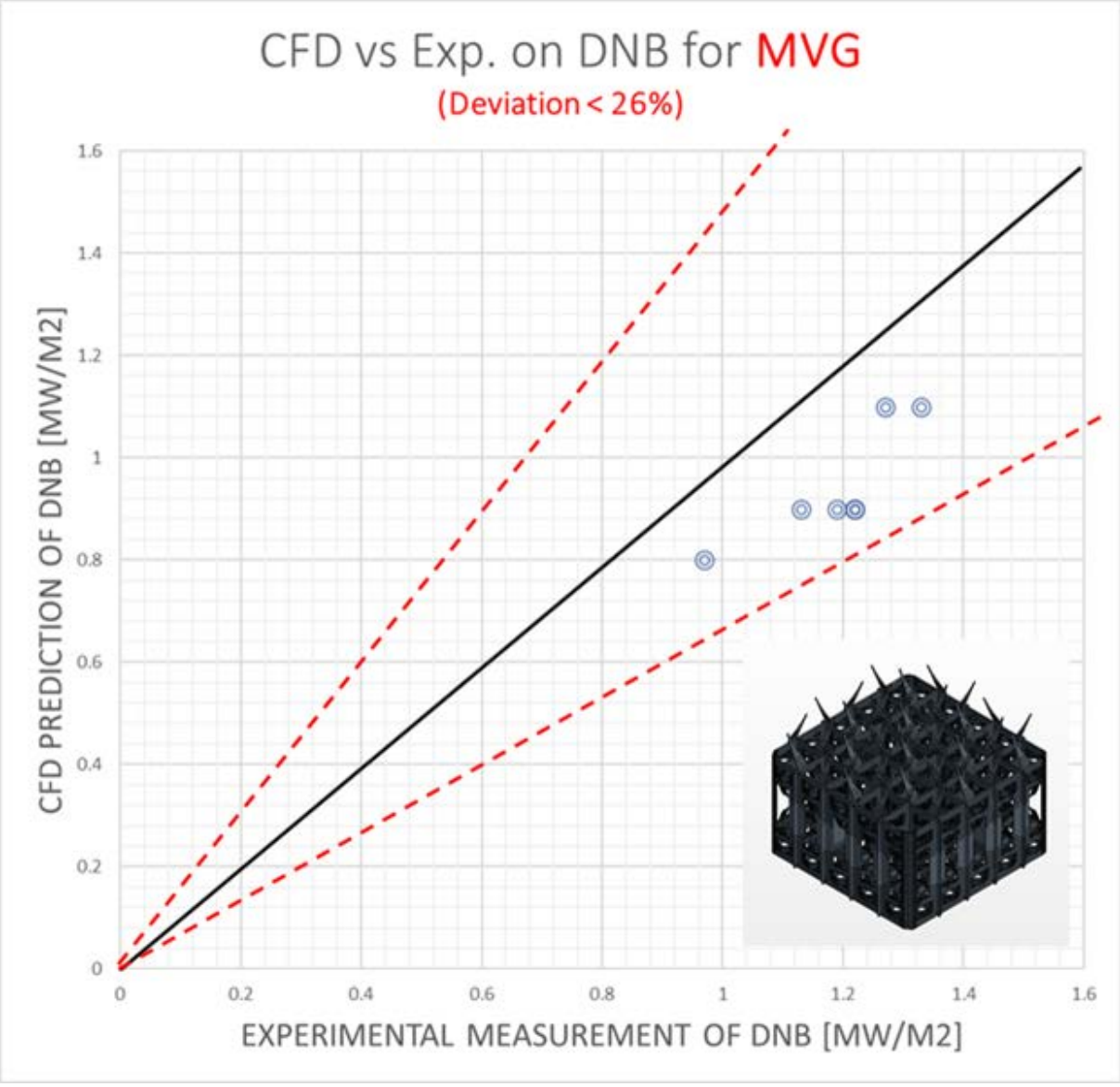

Figure 13 Predicted DNB vs measured DNB for Mixing Vane Grid (MVG) configuration

5. Conclusions and Future works

The main focus of the current study is to evaluate the predictive capability of the Generation-I boiling model for the 5x5 fuel bundle DNB application at a PWR-like operating condition. An incremental approach (simple pipe to complex fuel bundle with mixing vane) is applied to evaluate the maturity of the tested model and its DNB predictive capability. The baseline model is assessed by comparing the simulated DNB results with existing experimental DNB datasets. The preliminary result from various validation campaigns provide a best practice guideline for the DNB modeling in the sub-channel analysis. The findings can be reiterated as follows:

- A Multi-step validation framework with incrementally increasing complexity in the flow channels (e.g. single pipe to 5x5 fuel bundle with mixing vane grid) was developed and tested for the DNB performance.
- Reasonable DNB test matrices were down-selected after the assessment of the WEC DNB reports. 11 cases were selected for NMVG-DNB test matrix and 7 cases were selected for MVG-DNB test matrix.
- Three different meshes and five different lift coefficients were evaluated in terms of sensitivity of DNB prediction. Mesh sensitivity for DNB performance was not noticeably observed, but the lift model seems to have appreciable effect on the DNB prediction.
- Visualization of the high void fraction analysis presented in the current study could provide a useful insight to identify the potential DNB occurrence location along the length of the fuel rods.
- The DNB predictive capabilities with NMVG and MVG configuration were 16% and 26% respectively. It is still believed that the CASL baseline boiling model (GEN-1A) presents a reasonable DNB assessment for the 5x5 sub-channel application with good numerical robustness (i.e. no breakdown or divergence observed from the current study).

However, the current effort on the DNB validation study has also introduced fundamental questions for the next generation boiling model development. 1) More investigations on the lateral void fraction distribution-related boiling closure (lift and wall lubrication model), and 2) how to appropriately determine the DNB detection criteria within the premise of the current microlayer approach. In FY18, these limitations will be further investigated while demonstrating the improved boiling models (GEN-1B, GEN-2).

6. References

1. Seung Jun Kim, Emilio Baglietto, Etienne Demarly, LA-UR-16-28815, “Evaluation of DNB predictive capability in multiphase boiling model of STAR-CCM+”, L3.THM.CFD.P13.04
2. Emilio Baglietto, Seung Jun Kim, Etienne Demarly, LA-UR-16-29368, “Demonstration of DNB analysis methods using CFD”, L2.THM.P13.02
3. J. Weisman and B. S. Pei, Prediction of critical heat flux in flow boiling at low qualities, Int. J. Heuf Muss Transfer 26, 1463-1477 (1983).

Appendix A: Mixing effect visualization in NMVG and MVG

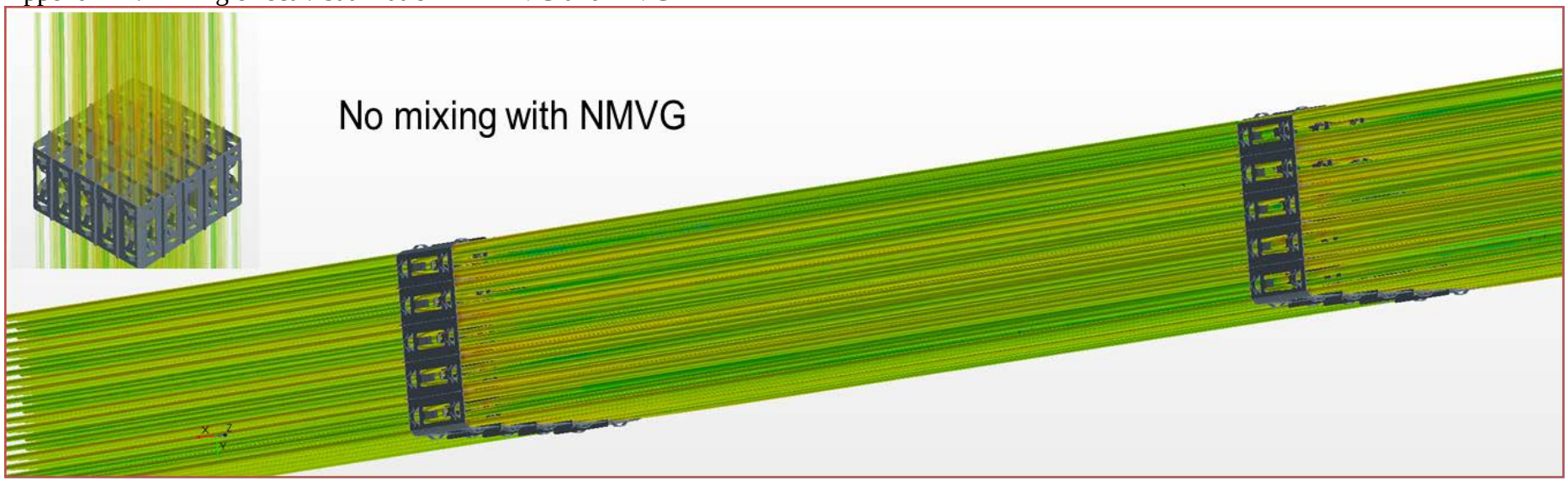

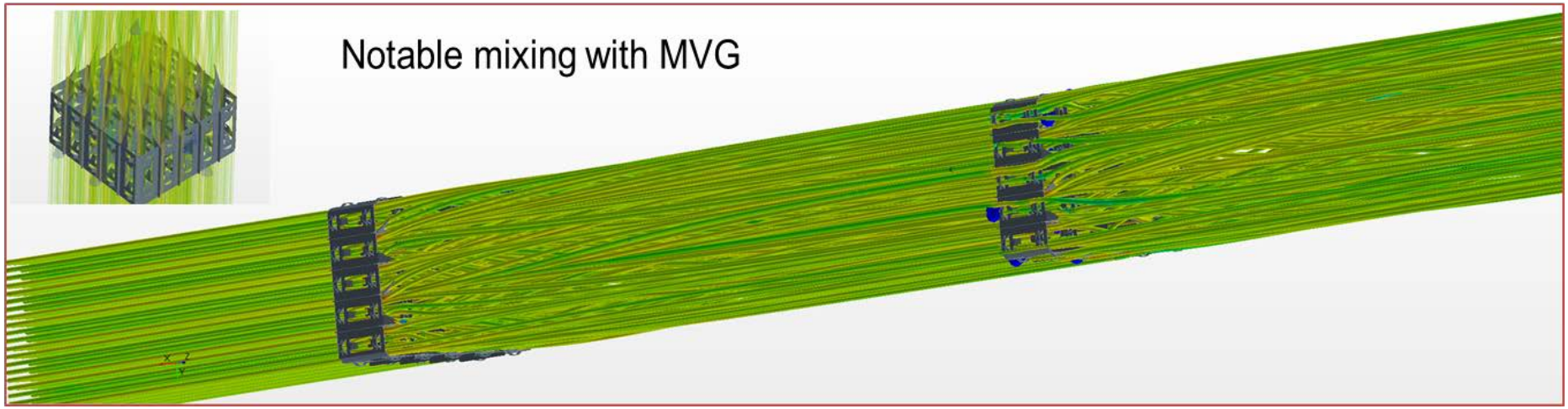

Appendix B: the effect of Lift model on DNB prediction

1. Lift coefficient effect on DNB with M1 (base size = 2mm, 21M)

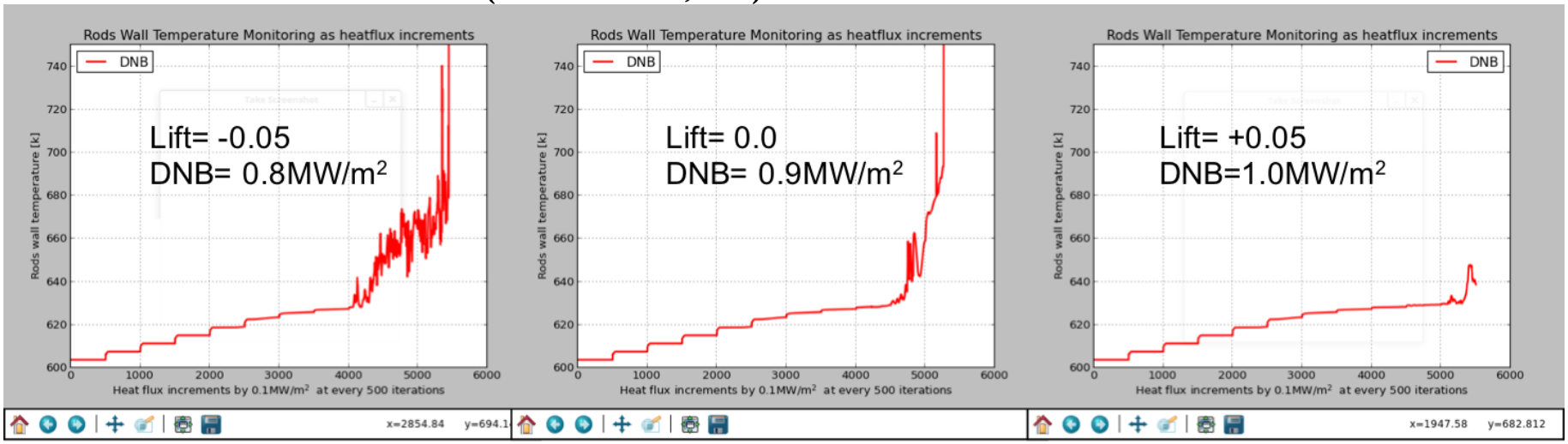

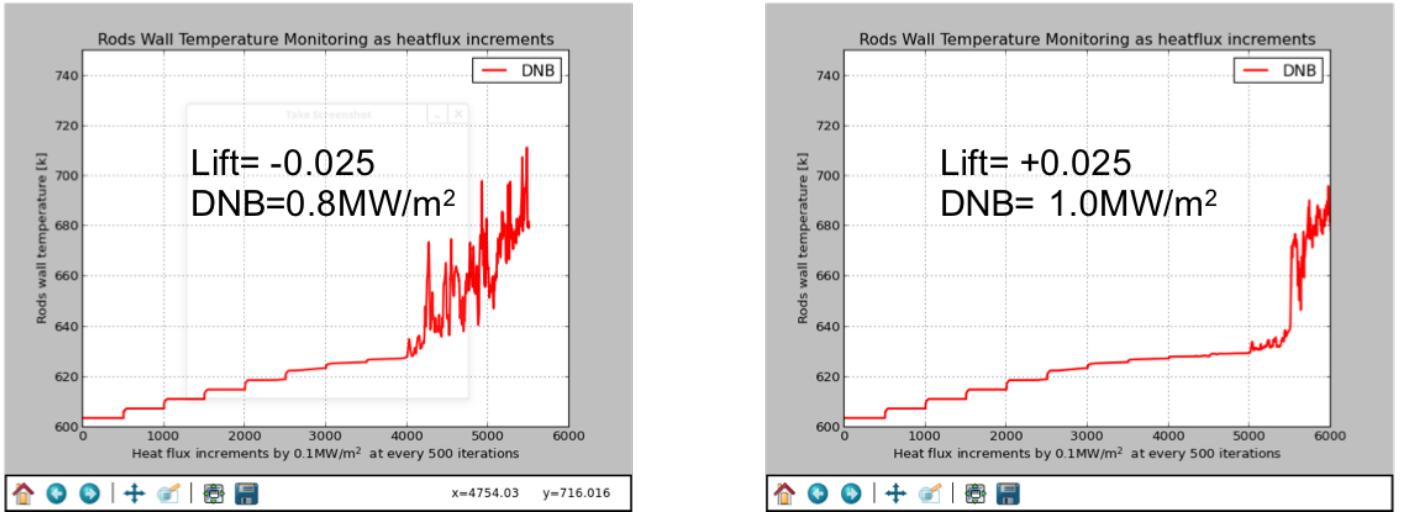

2. Lift coefficient effect on DNB with M2 (base size = 1mm, 35M)

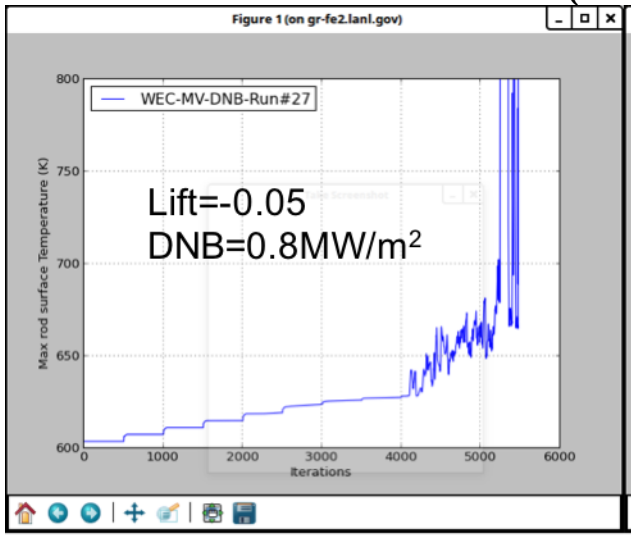

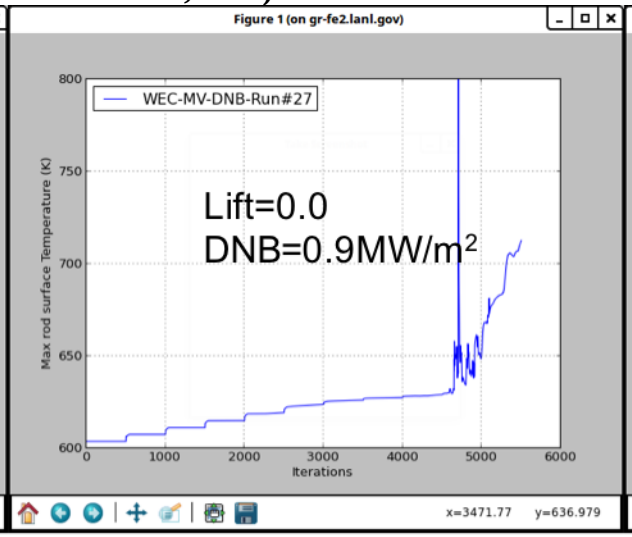

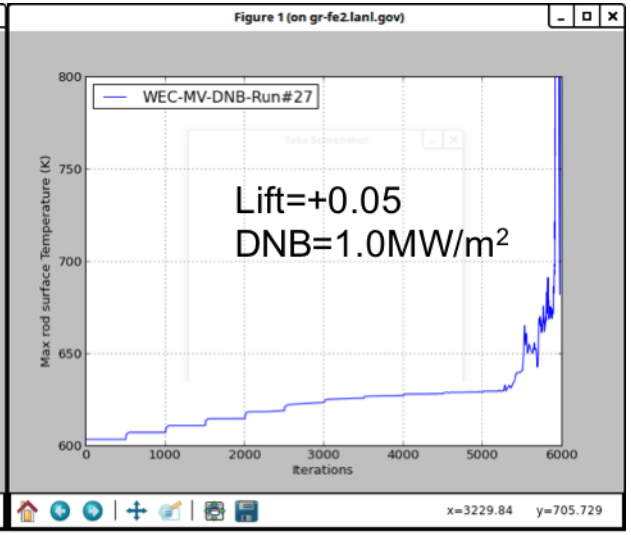

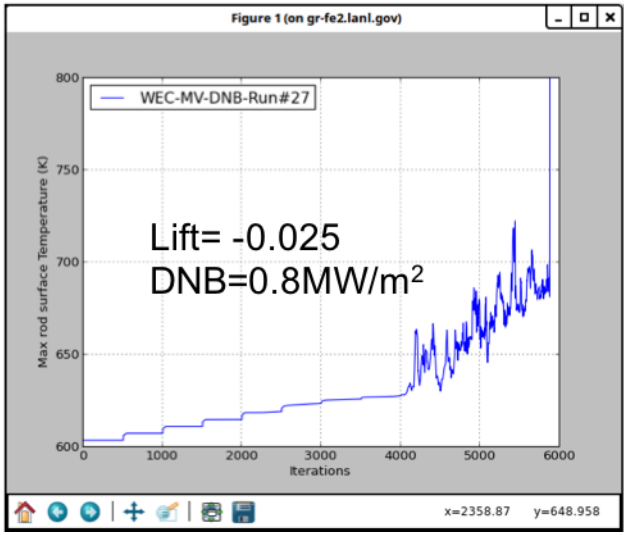

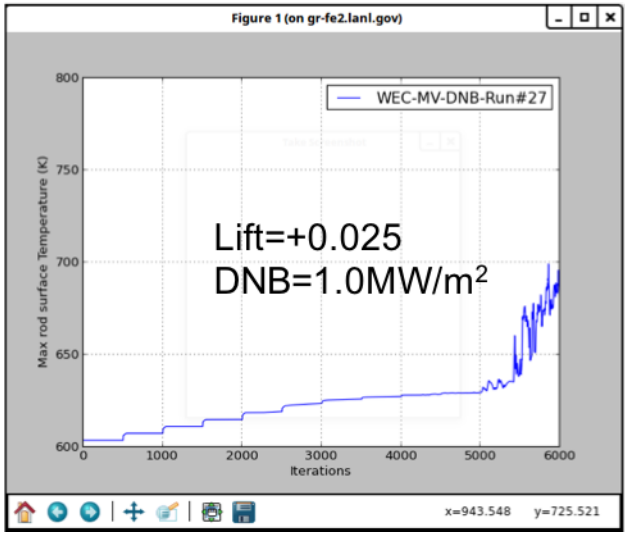

3. Lift coefficient effect on DNB with M3 (base size = 0.6mm, 73M)